Indian Journal of Pure & Applied Physics
Vol. 63, July 2025, pp. 638-647
DOI: 10.56042/ijpap.v63i7.19132

# Computational Analysis of MHD Copper-Water Nanofluid with effect of Viscous Dissipation & Thermal Radiation over Isothermal Moving Sheet

Shakshi Sharma & Susheela Chaudhary*

Department of Mathematics, Shri Kalyan Rajkiya Kanya Mahavidyalaya, Sikar 332 001, India

*Received: 25 April 2025; accepted: 4 June 2025*

The study has examined the flow of Cu-$H_2O$ nanofluid over an isothermal moving sheet subjected to the influence of viscous dissipation, thermal radiation and a vertical magnetic field. The fundamental partial differential equations have been transformed into a system of ordinary differential equations through the application of similarity transformation. The MATLAB tool 'bvp4c' has been employed to solve dimensionless ordinary differential equations to get numerical results. The effects of emerging parameters say velocity and temperature profiles have been depicted through graphs. With increase in volume fraction of particles, it shows an increasing tendency in the velocity curves for both the particle shapes taken. The pronounced elevation in temperature, driven by an increase in viscous dissipation (higher Eckart number) and platelet shape produces much higher temperature than spherical shapes. The values for Nusselt number for platelet shape exceeds the values of spherical shape particles. This work has applications in nanofluid-based cooling systems, thermal energy storage, magnetic field control, etc.

**Keywords:** Nanofluid, Magnetohydrodynamics (MHD), Viscous dissipation, Thermal radiation, Isothermal moving sheet

## 1 Introduction

Nanofluids represent a revolutionary class of engineered liquids, consisting of a base fluid (typically water, oil, or ethylene glycol) enhanced with nanoparticles of materials such as metals, oxides, or carbon-based substances lighted by Choi[1]. These nanoparticles, often in the size range of 1-100 nm, Among the myriad of potential nanofluid formulations, copper-water nanofluids have attracted considerable attention due to the superior thermal conductivity of copper nanoparticles. Many researchers worked on copper water nanofluid, some of the works are namely Lund *et al.*[2], Hayat *et al.*[3], Saleem *et al.*[4]. The presence of copper particles taking water as base fluid leads to a remarkable enhancement in the heat transfer properties of the base fluid, making it an ideal candidate for a variety of industrial applications, including those requiring high thermal efficiency. Copper, with its high thermal conductivity and relatively low cost, serves as an excellent nanoparticle material to enhance the thermal properties of water, resulting in a nanofluid that can significantly outperform conventional cooling fluids.

In the domain of scientific research, copper-water nanofluids have garnered significant attention due to their potential to enhance the efficiency of cooling systems. The shape of the nanoparticles plays a leading role in optimizing the flow characteristics, which in turn improves the overall performance. The impact of particle shape on the Cu-water Marangoni boundary layer flow, as well as its influence on radiation heat transfer within an electrically conducting, incompressible copper-water nanofluid subjected to an exponential temperature gradient, has been thoroughly examined by Chaudhary and Kanika[5]. The study aiming to delve into the effects of viscous dissipation, Joule heating and thermal radiation on the flow of a magneto-nanofluid between two horizontally aligned plates, as explored by Khan[6]. The investigation of combined influence of particle shape factors in the electrical MHD boundary layer flow of nanofluids, utilizing Buongiorno's model over a permeable linear stretching sheet, as discussed by Daniel *et al.*[7]. Additionally, Mohana and Kumar[8] have explored the effects of copper-water nanofluid utilizing the shape factor on boundary layer flow and heat transfer over a nonlinear stretching sheet in a porous medium.

MHD nanofluid flow is an innovative and rapidly evolving field that combines the advancements in nanofluid technology with the principles of magnetohydrodynamics to offer groundbreaking solutions in thermal management, energy systems, electronics cooling, and biomedical applications.

*Corresponding author: E-mail: susheelamaths@gmail.com

Waqas[9] worked on MHD water-based hybrid nanofluid flow over rotating disk indicating a complex geometry in itself. This investigation of Hayat *et al.*[10] addresses the MHD mixed convection flow of Casson flow over stretching cylinder. Ashwinkumar[11] examined the significance of nonlinear thermal radiation on MHD flow of hybrid nanofluid across two distinct geometries. Raza *et al.* [12] examined Hybrid Nanofluid Flow through Orthogonal Coaxial Porous Disks with influence of applied magnetic field.

The significance of viscous dissipation is further magnified in non-Newtonian fluids where viscosity varies with shear rate and in high-viscosity fluids, which exhibit greater resistance to flow. Viscous dissipation is the irreversible transformation of mechanical energy into thermal energy, occurring due to the internal friction between fluid layers when they move relative to one another. In such systems, the heat generated from frictional forces can no longer be ignored, making the effects of viscous dissipation critical to understanding the overall fluid behaviour. Mishra and Kumar[13] purposed to examine generative/absorptive heat and mass transfer magnetohydrodynamic flow past a wedge in order to explore fluid characteristics in presence of viscous dissipation through a porous medium. The study of MHD hybrid nanofluid is need of modern world because of its potential applications in modern engineering technologies, especially in improving thermal management and efficiency across a wide range of industrial processes and investigation of fluid flow considering the impact of viscous dissipation over a stretching surface is presented by Rehman *et al.* [14].

Thermal radiation is a fundamental mode of heat transfer that occurs mainly through the emission of electromagnetic waves and is a fundamental element of electronic and mechanical equipment. The understanding of radiation heat transfer is crucial for designing the appropriate equipment for various operations, especially in engineering and other specialized technological fields that involve extreme temperature conditions. Ali *et al.* [15] investigated about thermal properties of nanofluid flow considering heat radiation and heat generation/absorption. The characteristics of thermophoresis and Brownian motion in three-dimensional flow of nanofluid modeled in the presence of magnetic field by Shehzad *et al.* [16].

An isothermal moving sheet refers to a surface that maintains a constant temperature while moving at a specific velocity relative to the surrounding fluid. This idealized concept offers profound insights into the fundamental behaviours of fluids in motion and is widely utilized in modeling to examine the effects of thermal interactions, shear forces, and flow dynamics. For instance, Noghrehabadi *et al.* [17] presented a model of an isothermal moving sheet in the context of MHD dissipative nanofluids. Additionally, Ibrahim and Sanker[18] explored the boundary layer flow of nanofluid for observation of heat transfer characteristics over a non-isothermal stretching sheet, incorporating the effects of magnetic fields and thermal radiation. Moreover, Khan *et al.* [19] investigated a hybrid nanofluid non-stagnation point flow over a non-isothermal stretching/shrinking sheet, examining the influences of inertial forces and microstructural characteristics. Its utility in simplifying complex thermal and fluid dynamics processes, especially in heat transfer, through ongoing research and development, the understanding of isothermal moving sheets continues to contribute to innovations in energy efficiency, manufacturing, and technological advancements.

This investigation works to determine the parameters of radiation, viscous dissipation and velocity ratio to determine the flow of Cu-water nanofluid considering two particle shapes namely spherical and platelet. Using fundamental PDEs and appropriate transformation, ODEs of flow are modeled and solved using numerical scheme bvp4c. The results illustrate the impact of physical parameters on the flow characteristics, with graphical representations and physical quantities of interest are systematically presented in tabular form. A strong correlation between the present values and those found in the existing literature further validates the accuracy and reliability of the results.

**Nomenclature**

| | |
|---|---|
| $\sigma$ | Electric Conductivity |
| $Pr$ | Prandtl number |
| $C_p$ | Specific heat at constant pressure |
| $\rho C_p$ | Heat Capacity |
| $R$ | Radiation parameter |
| $Ec$ | Eckart number |
| $\psi$ | Stream function |
| $B_0$ | Magnetization of the permanent magnets |
| $Re_x$ | Local Reynolds number |

| | |
|---|---|
| $q_r$ | Radiative heat flux |
| $\kappa$ | Thermal conductivity |
| $\phi$ | Nanoparticles volume fraction |
| $\rho$ | Effective density |
| $M$ | Magnetic parameter |
| $\mu$ | Effective dynamic viscosity |
| $\eta$ | Similarity variable |
| $Re_x^{-\frac{1}{2}} C_f$ | Reduced skin friction coefficient |
| $Re_x^{\frac{1}{2}} Nu_x$ | Reduced Nusselt number. |

## 2 Mathematical Formulation

Considering two-dimensional, viscous, steady, incompressible, laminar boundary layer flow of an electrically conducting copper-water nanofluid with two different particle shapes say spherical and platelet over an isothermal moving sheet subjected to a uniformly distributed transverse magnetic field. The moving surface selected in a way that it moves in same or opposite direction of free stream with variable velocities. This model also takes into account thermal radiation and viscous dissipation. Here, u and $v$ are velocity components corresponding to x and y directions respectively. The free stream velocity is uniformly maintained at $U_\infty$ ($U_\infty > 0$) and velocity of fluid is maintained at $U_w$. If $U_w > 0$ implies motion of the plate in positive x- direction while $U_w < 0$ implies its motion in negative x-direction. The corresponding wall and ambient temperature of flow are maintained as $T_w$ and $T_\infty$ respectively where $T_w > T_\infty$. Under the virtue of above assumptions and schematic of flow geometry in Fig. 1, the required equations of flow are given by

$$\frac{\partial u}{\partial x} + \frac{\partial v}{\partial y} = 0 \quad \ldots (1)$$

$$u\frac{\partial u}{\partial x} + v\frac{\partial u}{\partial y} = \vartheta_{nf}\frac{\partial^2 u}{\partial y^2} - \frac{\sigma_{nf}B_0^2}{\rho_{nf}}u \quad \ldots (2)$$

$$\left(\rho C_p\right)_{nf}\left(u\frac{\partial T}{\partial x} + v\frac{\partial T}{\partial y}\right) = \kappa_{nf}\frac{\partial^2 T}{\partial y^2} - \frac{\partial q_r}{\partial y} + \mu_{nf}\left(\frac{\partial u}{\partial y}\right)^2 \quad \ldots (3)$$

Subjected with the boundary conditions-

$$\left.\begin{array}{l} y = 0: u = u_w, v = 0, T = T_w \\ y \to \infty: u \to U_\infty, T \to T_\infty \end{array}\right\} \quad \ldots (4)$$

The considered Heat flux is presented by Rosseland Approximation as under

$$q_r = -\frac{4\sigma^*}{3k^*}\frac{\partial T^4}{\partial y} = -\frac{16\sigma^*}{3k^*}T_\infty^3\frac{\partial T}{\partial y} \quad \ldots (5)$$

Here, $\sigma^*$ is the Stefan-Boltzmann constant and $k^*$ stands for the coefficient of mean absorption. By putting this value in equation (4), we have

$$\left(\rho C_p\right)_{nf}\left(u\frac{\partial T}{\partial x} + v\frac{\partial T}{\partial y}\right) = (\kappa_{nf} + \frac{16\sigma^*}{3k^*}T_\infty^3)\frac{\partial^2 T}{\partial y^2} + \mu_{nf}\left(\frac{\partial u}{\partial y}\right)^2 \quad \ldots (6)$$

Further, The thermophysical properties of nanofluids are given by Waqas *et al.* [20]

$$\left.\begin{array}{l} \frac{\mu_{nf}}{\mu_f} = 1 + S_1\phi + S_2\phi^2 \\ \frac{\rho_{nf}}{\rho_f} = (1-\phi) + \phi\left(\frac{\rho_s}{\rho_f}\right) \\ \frac{\kappa_{nf}}{\kappa_f} = \frac{(n-1)\kappa_f + \kappa_s + (n-1)\phi(\kappa_s - \kappa_f)}{(n-1) + \kappa_s - \phi(\kappa_s - \kappa_f)} \\ \frac{(\rho C_p)_{nf}}{(\rho C_p)_f} = (1-\phi) + \phi\left(\frac{(\rho C_p)_s}{(\rho C_p)_f}\right) \end{array}\right\} \quad \ldots (7)$$

Here, subscript s, f and nf indicates the physical properties of solid nano particles, base fluid and nanofluid respectively and $\phi$ here indicates the volume fractions of solid nanoparticles. The

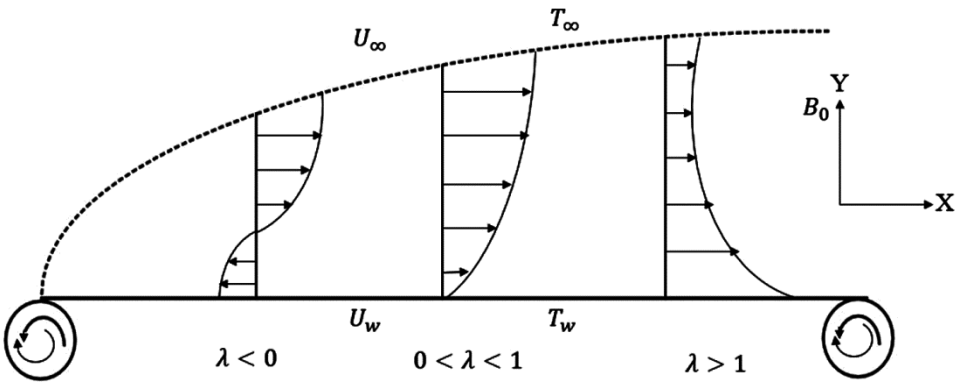


Fig. 1 — Schematic of flow geometry

thermophysical properties of Cu-$H_2O$ nanofluids are given in Table 1. (Malvandi *et al.* [21]).

The viscosity coefficients ($S_1$ and $S_2$) are given in Table 2 for spherical and platelet shapes and the sphericity ($\varsigma$) and shape factor (n) for the spherical and platelet shapes are given in Table 3 by Waqas *et al.* [20].

## 3 Similarity Transformation

In order to transform the governing PDE's of flow into non-dimensional ODE's, the following Stream function ($\psi$), Similarity variable ($\eta$), Temperature ($T$) and corresponding velocities for copper-water nanofluid are given as

$$\left.\begin{aligned}\psi = \sqrt{2\nu_f U_\infty x}\, f(\eta), \eta = \sqrt{\frac{U_\infty}{2\nu_f x}}\, y, T = (T_w - T_\infty)\theta(\eta) + T_\infty \\ u = U_\infty f'(\eta), v = \frac{U_\infty y}{2x} f'(\eta) - \sqrt{\frac{\nu_f U_\infty}{2x}} f(\eta)\end{aligned}\right\} \quad \ldots (8)$$

Here, the above equation (8) satisfies equation (2) that gives $u = \frac{\partial \psi}{\partial y}$, $v = -\frac{\partial \psi}{\partial x}$ and it reduce the momentum and energy equations in the following manner.

$$f''' + \left(\frac{\rho_{nf}}{\rho_f}\right)\left(\frac{\mu_f}{\mu_{nf}}\right) f f'' - \left(\frac{\mu_f}{\mu_{nf}}\right) M f' = 0 \quad \ldots (9)$$

$$\left(\frac{\kappa_{nf}}{\kappa_f} + R\right)\theta'' + \left(\frac{(\rho C_p)_{nf}}{(\rho C_p)_f}\right) \Pr f\theta' + Ec. \Pr \left(\frac{\mu_{nf}}{\mu_f}\right) f''^2 = 0 \quad \ldots (10)$$

Which gives the following boundary conditions:

Table 1 — Thermophysical properties of various materials used in the present study

| Properties | Copper | Water |
|---|---|---|
| $\rho(Kgm^{-3})$ | 8933 | 997.1 |
| $\kappa(Wm^{-1}K^{-1})$ | 400 | 0.613 |
| $C_p(JKg^{-1}K^{-1})$ | 385 | 4179 |

Table 2 — Specific values of the viscosity coefficients ($S_1$ and $S_2$) used in the present study

| Viscosity Coefficients | Sphere | Platelet |
|---|---|---|
| $S_1$ | 2.5 | 37.1 |
| $S_2$ | 6.2 | 612.6 |

Table 3 — Specific values of sphericity ($\psi$) and shape factor (n) used in the present study

| Properties | Sphere | Platelet |
|---|---|---|
| sphericity ($\varsigma$) | 1 | 0.52 |
| shape factor (n) | 3 | 5.77 |

$$\left.\begin{aligned}\eta = 0: f(0) = 0, f'(0) = \lambda = \frac{U_w}{U_\infty}, \theta(0) = 1 \\ \eta \to \infty: f'(\infty) \to 1, \theta(\infty) \to 0\end{aligned}\right\} \quad \ldots (11)$$

where, $M = \frac{2x\,\sigma_{nf} B_0^2}{U_\infty \rho_f}$ is the magnetic parameter, $R = \frac{16\sigma^* T_\infty^3}{3k^* \kappa_f}$ is the radiation parameter, $Pr = \frac{\mu_f (C_p)_f}{\kappa_f}$ is the Prandtl number, $Ec = \frac{{U_\infty}^2}{(T_w - T_\infty)(C_p)_f}$ is the Eckart number and $\lambda = \frac{U_w}{U_\infty}$ is the velocity ratio or moving parameter.

## 4 Manifesto of Investigation

The experimental quantities of interest are skin friction coefficient ($C_f$) and Nusselt number ($Nu_x$) and are given by below expression

$$C_f = \frac{2\tau_w}{\rho_f {U_\infty}^2}, Nu_x = \frac{x q_w}{\kappa_f (T_w - T_\infty)} \quad \ldots (12)$$

$\tau_w$ and $q_w$ here represents the heat flux and wall shear stress respectively and are given by

$$\tau_w = \mu_{nf}\left(\frac{\partial u}{\partial y}\right)_{y=0}, q_w = -\kappa_{nf}\left(\frac{\partial T}{\partial y}\right)_{y=0} \quad \ldots (13)$$

Using Eqs (12) and (13), the expression for dimensionless skin friction coefficient and Nusselt number are given by

$$\left.\begin{aligned}Re_x^{-\frac{1}{2}} C_f = \sqrt{2}\left(\frac{\mu_{nf}}{\mu_f}\right) f''(0) \\ Re_x^{\frac{1}{2}} Nu_x = -\frac{1}{\sqrt{2}}\left(\frac{\kappa_{nf}}{\kappa_f}\right)\theta'(0)\end{aligned}\right\} \quad \ldots (14)$$

Here, $Re = \frac{U_\infty x}{\nu_f}$ is the expression for local Renyolds number, $f''(0)$ and $\theta'(0)$ represents surface stress and surface heat flux respectively.

## 5 Numerical Solution and Validation

For the above problem taking Prandtl number ($Pr = 6.2$), selected values of velocity ratio parameter, magnetic parameter, radiation parameter, nanoparticle volume fraction, Eckart number considering two different particle shapes of copper-water nanofluid implementing in MATLAB's inbuilt boundary layer problem solver method (bvp4c), achieve the solution of Eqs (9) and (10) with boundary conditions (11). The selection of the value at infinity boundary position which has to be optimal, is taken to be $n \to \infty = 10$ occupied for

computational step size $\Delta\eta = 10^{-3}$. The Boundary value problem equations are transformed to first order equations for the numerical procedure as given by

$$e(1) = f(\eta)\,, \quad e(2) = f'(\eta)\,, \quad e(3) = f''(\eta)\,, \quad e(4) = \theta(\eta)\,, e(5) = \theta'(\eta) \qquad \ldots (15)$$

Now, equations are given by

$$\begin{bmatrix} e'(1) \\ e'(2) \\ e'(3) \\ e'(4) \\ e'(5) \end{bmatrix} = \begin{bmatrix} e(2) \\ e(3) \\ \frac{M}{1+S_1\phi+S_2\phi^2}\, e(1) - \frac{(1-\phi)+\phi\left(\frac{\rho_S}{\rho_f}\right)}{1+S_1\phi+S_2\phi^2}\, e(1)\, e(3) \\ e(5) \\ \frac{-\left\{(1-\phi)+\phi\left(\frac{(\rho C_p)_S}{(\rho C_p)_f}\right)\right\} e(1)\, e(5)\, Pr - \{1+S_1\phi+S_2\phi^2\}\, PrEc\,(e(3))^2}{\frac{(n-1)\kappa_f+\kappa_S+(n-1)\phi(\kappa_S-\kappa_f)}{(n-1)+\kappa_S-\phi(\kappa_S-\kappa_f)}+R} \end{bmatrix} \qquad \ldots (16)$$

And initial circumstances are given by

$$\begin{bmatrix} e_a(1) \\ e_a(2) \\ e_a(4) \\ e_b(2) \\ e_b(4) \end{bmatrix} = \begin{bmatrix} 0 \\ \lambda \\ 1 \\ 1 \\ 0 \end{bmatrix} \qquad \ldots (17)$$

The comparison of results obtained with that of obtained by Chaudhary[22] taking the spherical shaped particles and considering value of $Pr = 6.2$ and $\phi = 0.08$ are found to be in excellent correlation as shown in Table 4.

## 6 Results and Discussion

Employing the efficient MATLAB's inbuilt boundary value problem solver-bvp4c, coupled with consistent guessing, the governing Eqs (9) and (10), taking in account their respective boundary conditions in (11), are solved numerically. A range of factors defining the flow are subjected to computational analysis, and the resulting outcomes are presented through graphical representations.

Figure 2(a-b) demonstrate the variation of velocity parameter with velocity ratio parameter, it depicts that the velocity distribution rises with increase in value of $\lambda$ for both particle shapes. Here the flow is analysed for three different cases of $\lambda$ such as $\lambda < 0, 0 < \lambda < 1$ and $\lambda > 1$ as shown in Fig. 1. The velocity ratio parameter assumes values greater than zero when the plate moves in the direction of the free stream. When $0 < \lambda < 1$, the plate's motion is slower than the velocity of the nanofluid. As $\lambda$ approaches unity, the boundary layer becomes thinner. However, an increase in the boundary layer thickness occurs as $\lambda$ exceeds unity ($\lambda > 1$), when the plate's velocity

Table 4 — Comparison of values of $f''(0)$ and $\theta'(0)$.

| $\lambda$ | $-f''(0)$ | | $-\theta'(0)$ | |
|---|---|---|---|---|
| | Chaudhary[22] | Present Result | Chaudhary[22] | Present Result |
| -0.3 | -0.41869 | -0.417616 | 0.322559 | 0.321436 |
| -0.1 | -0.53200 | -0.532765 | 0.704170 | 0.704806 |
| 0.1 | -0.53329 | - 0.533442 | 0.970043 | 0.970247 |
| 1.5 | 0.52764 | 0.527001 | 2.077050 | 2.077279 |

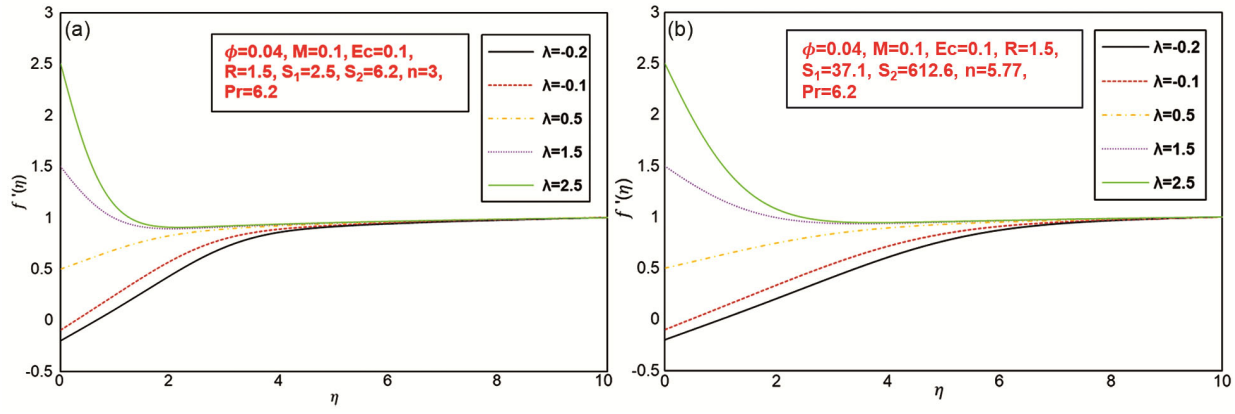


Fig. 2 (a) — Velocity profile Vs Velocity ratio parameter for spherical shape particle; (b) Velocity profile Vs Velocity ratio parameter for platelet shape particles

surpasses that of the free stream. This phenomenon is attributed to the pulling force exerted by the plate on the fluid, which reverses the direction of the frictional force, resulting in an expansion of the boundary layer. Velocity boundary layer thickness was found to be elevated for $\lambda < 0$ and it dropped for $\lambda > 0$. The velocity profile curve for spherical particle converges before the platelet shaped particle.

Figure 3 (a-b) depict the variation of temperature profiles with velocity ratio parameter, it shows decline of temperature distribution with rise in value of $\lambda$ for both the spherical and platelet particle shapes. As the velocity ratio parameter rises, the fluid is stretched and accelerated, leading to a thinner thermal boundary layer and enhanced convective heat transfer, which in turn causes the temperature of the nanofluid to decrease.

Figure 4 (a-b) demonstrate the variation of velocity profile with volume fraction of particles. With increase in volume fraction of particles, there is an increasing tendency in the velocity curves for both the particle shapes taken. This clearly mentions that platelet shaped particles have higher velocity profiles compared to spherical shaped particles.

Figure 5 (a-b) portray the variation of fluid's temperature profile with volume fraction of particles. The temperature of fluid upsurges with an increment in the volume fraction for the observed particle shapes of Cu-water nanofluid. It is due to insertion of more nanoparticles that boosts the thermal conductivity leading to the increment in temperature.

Figure 6 (a-b) show the influence of magnetic parameter which is associated to magnetic field on velocity boundary layer profile. The images shows that velocity boundary layer thickens as M grows. The physical impact of increasing M is that the boundary layer thickens as a result frictional resistance increases leading to decrease in the speed of fluid flow.

Figure 7(a-b) depict the behaviour of magnetic parameter on thermal profile of Cu-water nanofluid.

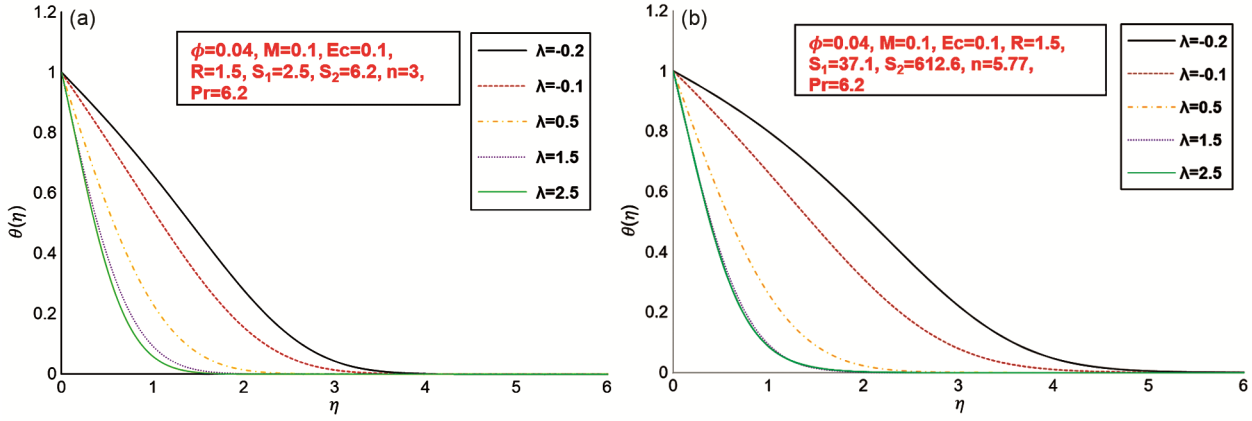


Fig. 3 (a) — Temperature profile Vs Velocity ratio parameter for spherical shape particles; (b) Temperature profile Vs Velocity ratio parameter for platelet shape particles

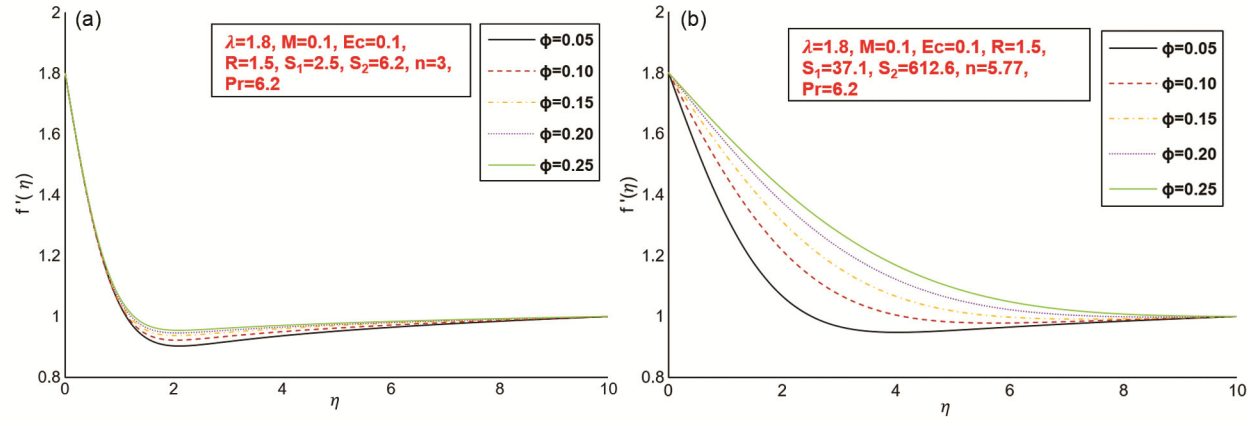


Fig. 4 (a) — Velocity profile Vs Volume fraction of particles for spherical shape particles; (b) Velocity profile Vs Volume fraction of particles for platelet shape particles

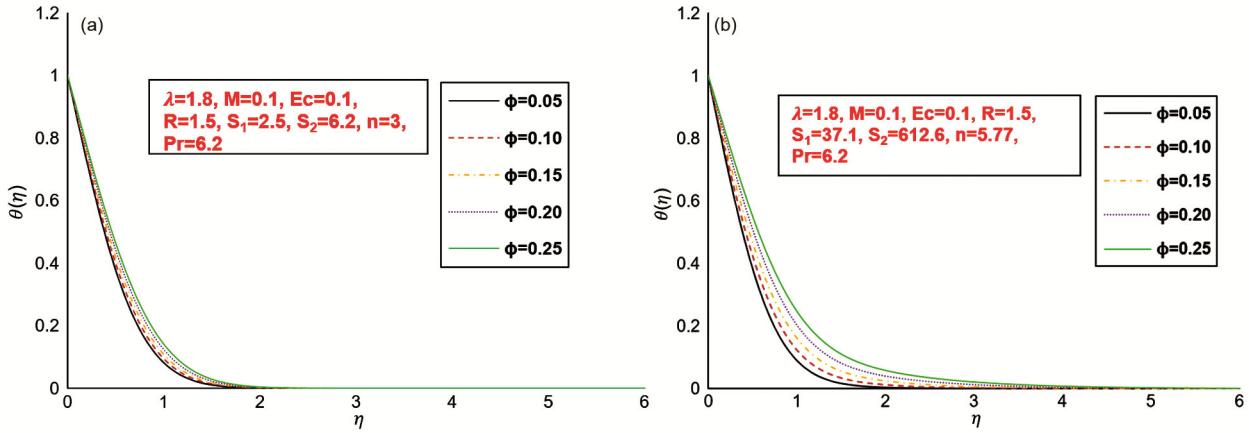


Fig. 5 (a) — Temperature profile Vs Volume fraction of particles for spherical shape particles; (b) Temperature profile Vs Volume fraction of particles for platelet shape particles

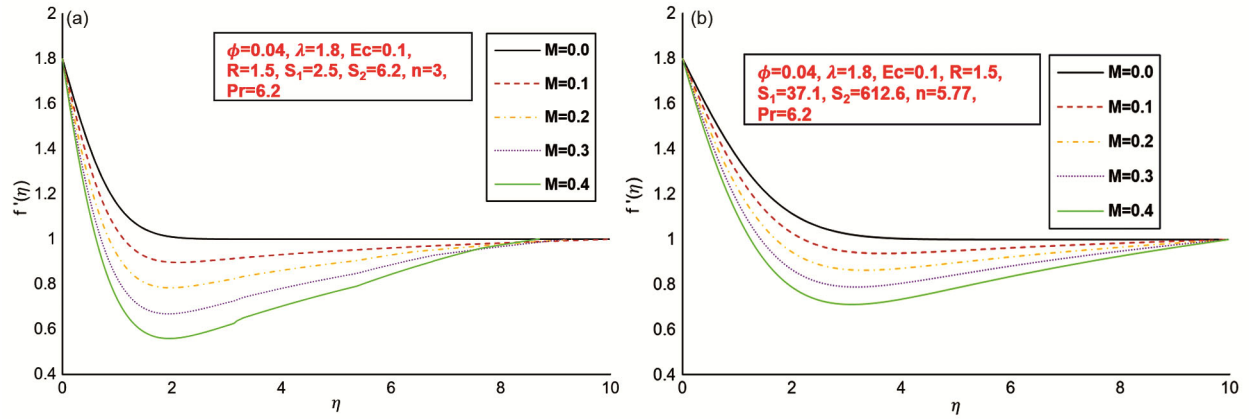


Fig. 6 (a) — Velocity profile Vs Magnetic parameter for spherical shape particles; (b) Velocity profile Vs Magnetic parameter for platelet shape particles

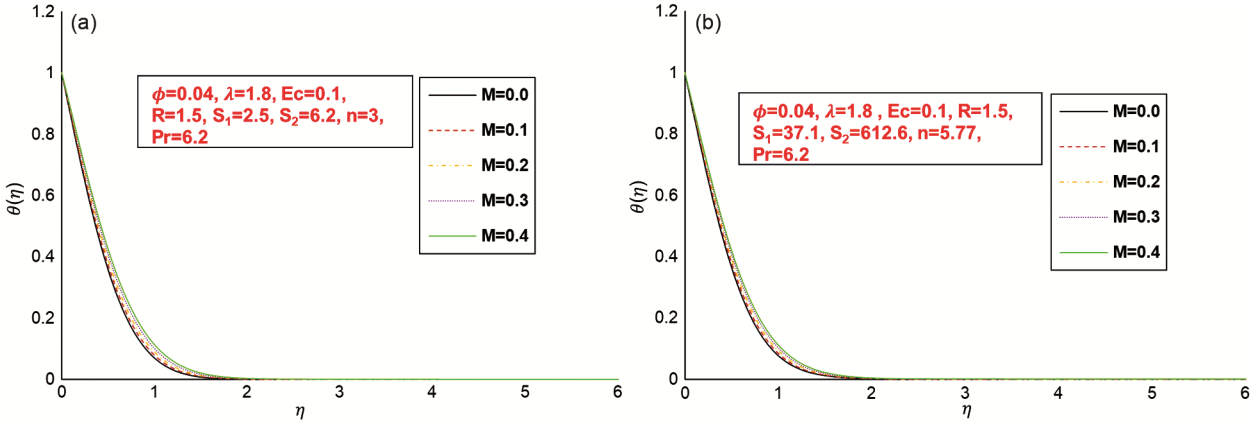


Fig. 7 (a) — Temperature profile Vs Magnetic parameter for spherical shape particles; (b) Temperature profile Vs Magnetic parameter for platelet shape particles

As the value of magnetic parameter rises, the thermal profile also increases. It indicates more the thermal boundary layer thickness less the heat transfer rate and creates more temperature difference within the fluid.

Figure 8(a-b) illustrate the effect of radiation parameter behaviour on the thermal profile of the Cu-water nanofluid. The graph clearly illustrates that the temperature profiles increase with increase of R. Physically, in existence of thermal radiation

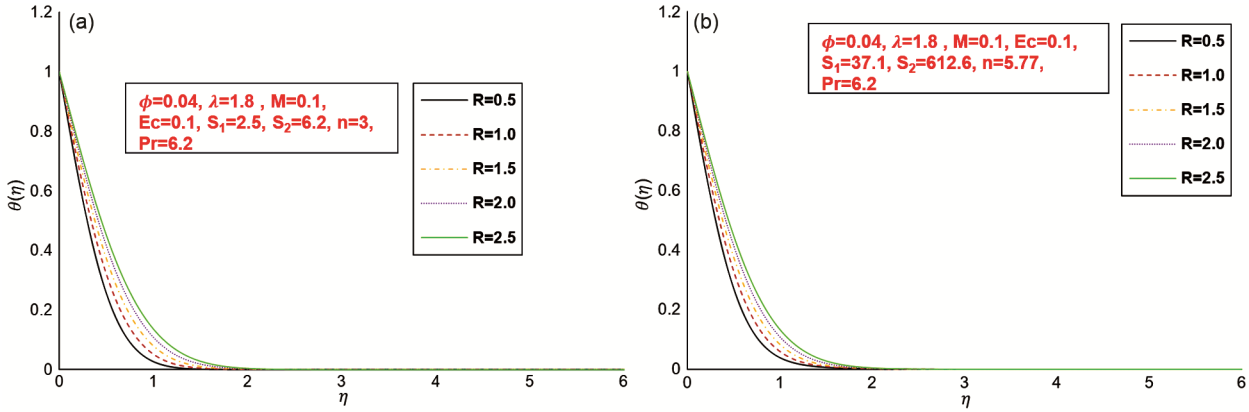


Fig. 8 (a) — Temperature profile Vs Radiation parameter for spherical shape particles; (b) Temperature profile Vs Radiation parameter for platelet shape particles

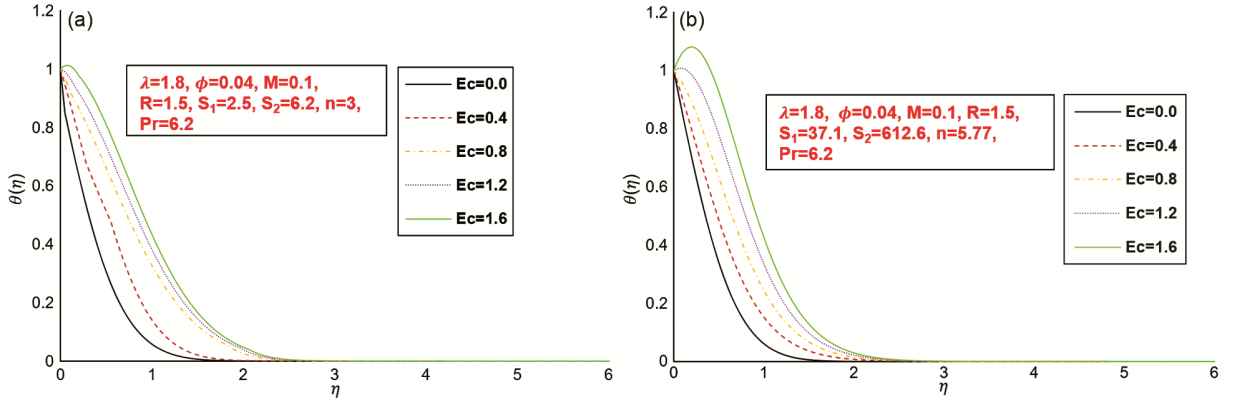


Fig. 9 (a) — Temperature profile Vs Eckart number for spherical shape particles, and (b) Temperature profile Vs Eckart number for platelet shape particles

significance increment in radiative heat, which assists in increasing the thermal of nanofluid, initiating its temperature to increase.

Figure 9(a-b) present how the Eckart number affects the thermal boundary layer profile. In these profiles, an increase in the Eckart number boosts the temperature curves for both the particle shapes. The pronounced elevation in temperature, driven by an increase in viscous dissipation (higher Eckart number), which directly contributes to internal heating of the fluid, platelet shape produces much higher temperature than spherical shapes. Here, platelet shaped particle shows an effective role in temperature distribution.

Table 5 presents the computed results of $(-Re_x^{-\frac{1}{2}}C_f)$ with variation in values of $\lambda$, $\phi$ and $M$ for Cu-water nanofluid for two different particle shapes say spherical and platelet. The local skin friction coefficient which is linked to the surface shear stress where a positive surface shear stress signifies a drag force exerted by the nanofluid on the plate and a negative surface shear stress indicates a force in the opposite direction. On enhancing values of $\phi$ and $M$, the Nusselt number enhances more for platelet shape particles as compared to spherical shaped particles.

The computed values of Table 6 clearly depicts that the values of Nusselt number decreases when we increase the value of velocity ratio parameter for velocity ratio parameter in negative x-direction and it has higher values for spherical shape than platelet shape and it tend to platelet than spherical as the velocity ratio parameter turns positive. Also, Nusselt number starts increasing with increase of velocity ratio parameter in positive direction. When we increase volume fraction of particles Nusselt number enhances more for platelet shape than spherical shaped particles. With the upgradation in magnetic parameter degradation of Nusselt number observed. In this case, the values of Nusselt number for platelet shape exceeds the values of spherical shape particles and the values decline on enhancement of both the Eckart number and radiation parameter.

Table 5 — Results of Skin friction coefficient for certain values of physical parameters for two particle shapes for $Pr = 6.2$

| $\lambda$ | $\phi$ | $M$ | $-Re_x^{-\frac{1}{2}}C_f$ | |
|---|---|---|---|---|
| | | | Spherical | Platelet |
| -0.2 | 0.04 | 0.1 | -0.612951 | -1.578958 |
| -0.1 | | | -0.650590 | -1.535543 |
| 0.1 | | | -0.634048 | - 1.380197 |
| 0.5 | | | -0.378809 | -0.823947 |
| 1.8 | 0.10 | | 1.932884 | 5.539790 |
| | 0.15 | | 2.248540 | 8.765395 |
| | 0.20 | | 2.586064 | 12.82930 |
| | 0.04 | 0.2 | 1.810807 | 3.012587 |
| | | 0.3 | 2.029855 | 3.314407 |
| | | 0.4 | 2.238050 | 3.606347 |

Table 6 — Results of Nusselt number for certain values of physical parameters for two particle shapes for $Pr = 6.2$

| $\lambda$ | $\phi$ | $M$ | $Ec$ | $R$ | $Re_x^{\frac{1}{2}}Nu_x$ | |
|---|---|---|---|---|---|---|
| | | | | | Spherical | Platelet |
| -0.2 | 0.04 | 0.1 | 0.1 | 1.5 | 0.282406 | 0.205596 |
| -0.1 | | | | | 0.370565 | 0.301039 |
| 0.1 | | | | | 0.460590 | 0.397165 |
| 0.5 | | | | | 0.744911 | 0.774234 |
| 1.8 | 0.10 | | | | 1.251054 | 1.438087 |
| | 0.15 | | | | 1.358222 | 1.539242 |
| | 0.20 | | | | 1.469206 | 1.567623 |
| | 0.04 | 0.2 | | | 1.095378 | 1.207884 |
| | | 0.3 | | | 1.062694 | 1.182363 |
| | | 0.4 | | | 1.029332 | 1.156030 |
| | | | 0.4 | | 0.883494 | 0.888731 |
| | | | 0.8 | | 0.558787 | 0.430464 |
| | | | 1.2 | | 0.234080 | 0.028022 |
| | | | | 1.0 | 1.255941 | 1.361836 |
| | | | | 2.0 | 1.030067 | 1.133709 |
| | | | | 2.5 | 0.953737 | 1.055144 |

## 7 Conclusion

The flow of dissipative Cu-water nanofluid flow over isothermal moving sheet in thermal radiation and applied magnetic field is observed theoretically in this article. A modified formulation for viscosity of different particle shapes is taken in consideration for the studied nanofluid. Two particle shapes- Spherical and Platelet are considered for comparison under various non-dimensional parameters. The Computation shows that

- The thickness of velocity boundary layer was observed to be heightened for values of $\lambda < 0$, whereas it diminished for $\lambda > 0$. Additionally, the velocity profile for spherical particles reaches convergence sooner than that for platelet-shaped particles. Also, the thermal boundary layer diminishes for increment of $\lambda$.
- Both the velocity and thermal boundary layer thickness widens for increment in $\phi$.
- With the rise of magnetic parameter, velocity and thermal profiles elevates.
- The upsurge in Eckart number and radiation parameter enhances thermal profiles.
- With an increase in the values of $\phi$ and M, the Nusselt number experiences a more pronounced enhancement for platelet-shaped particles in comparison to spherical-shaped particles, demonstrating a significantly superior thermal performance in the former.
- The Nusselt number for particles with a platelet shape surpasses that of spherical-shaped particles, indicating a more efficient heat transfer.
- The local Nusselt number decreases as the magnetic parameter, Eckart number and the

radiation parameter are increased and enhances with increased volume fraction of particles.

**Acknowledgment**

Shakshi Sharma (09/1368(15514)/2022-EMR-I) is grateful to CSIR, New Delhi, for financial assistance as a Senior Research Fellowship.

**References**

1 Choi S U S, *ASME Publ Fed*, 231 (1995) 99.
2 Lund L A, Omar Z, Khan I, Seikh A H, Sherif E S & Nisar K S, *J Mater Res Technol*, 9 (2020) 421.
3 Hayat T, Farooq S, Alsaedi A & Ahmad B, *Int J Heat Mass Transf*, 103 (2016) 1133.
4 Saleem S, Qasim M, Alderremy A & Noreen S, *Phys Scr*, 95 (2020) 055209.
5 Chaudhary S & Kanika K M, *Int J Comput Math*, 97 (2020) 943.
6 Khan U, Abbasi A, Ahmed N & Mohyud-Din S T, *Eng Comput*, 34 (2017) 2479.
7 Daniel Y S, Aziz Z A, Ismail Z & Salah F, *Chin J Phys*, 55 (2017) 630.
8 Mohana C M & Kumar B R, *Zeitschrift für Angewandte Mathematik und Mechanik*, 104 (2024) e202300188.
9 Waqas H, Farooq U, Naseem R, Hussain S & Alghamdi M, *Case Stud Therm Eng*, 26 (2021) 101015.
10 Hayat T, Khan M I, Waqas M, Yasmeen T & Alsaedi A, *J Mol Liq*, 222 (2016) 47.
11 Ashwinkumar G P, Samrat S P & Sandeep N, *Int Commun Heat Mass Transf*, 127 (2021) 105563.
12 Raza Q, Qureshi M Z, Ali B, Hussein A K, Khan B A, Shah N A & Weera W, *Mathematics*, 10 (2022) 3280.
13 Mishra A & Kumar M, *Heat Transf*, 50 (2021) 8453.
14 Rehman A, Khan D, Mahariq I, Elkotb M A & Elnaqeeb T, *J Mol Liq*, 408 (2024) 125370.
15 Ali U, Malik M Y, Alderremy A A, Aly S & Rehman K U, *Physica A Stat Mech Appl*, 553 (2020) 124026.
16 Shehzad S A, Hayat T, Alsaedi A & Obid M A, *Appl Math Comput*, 248 (2014) 273.
17 Noghrehabadi A, Ghalambaz M & Ghanbarzadeh A, *J Thermophys Heat Transf*, 26 (2012) 686.
18 Ibrahim W & Shanker B, *J Heat Transfer*, 136 (2014) 051701.
19 Khan U, Zaib A, Bakar S A & Ishak A, *Case Stud Therm Eng*, 26 (2021) 101150.
20 Waqas M, Kausar M S, Bég O A, Kuharat S, Khan W A, Abdullaev S S & Fadhl B M, *Int J Hydrog Energy*, 48 (2023) 34536.
21 Malvandi A, Ganji D D, Hedayati F & Rad E Y, *Alex Eng J*, 52 (2013) 595.
22 Chaudhary S, *Indian J Chem Technol*, 29 (2022) 311.